

# FULL WAVEFORM INVERSION IN AN ANISOTROPIC EARTH: A PRACTICAL WORKFLOW

T. Allemand<sup>1</sup>, A. Sedova<sup>1</sup>, G. Lambaré<sup>1</sup>, D. Grenié<sup>2</sup>, P. Guillaume<sup>1</sup>

<sup>1</sup> CGG; <sup>2</sup> previously in CGG

## Summary

---

An incorrect anisotropy in the Full Wave Inversion (FWI) velocity model leads to imperfect Common Image Gather (CIG) flatness. The main difficulty in the anisotropy estimation through FWI is the strong coupling with velocity. While FWI jointly updating velocity and anisotropy has been proposed, there is evidence that the long wavelength components of the velocity and anisotropic parameters cannot be reasonably decoupled inverting surface data only. The reason is that the long wavelength components of the velocity model inverted by FWI are mainly recovered from the kinematics of diving waves, while decoupling can only be done considering in addition the kinematics of reflected waves. To solve this challenge, we propose an innovative workflow involving joint reflection and diving wave tomography. To overcome the difficulty of first break picking, we propose a robust estimation of first arrival traveltimes using the inverted FWI model of the first pass. With the application of this novelty on deep-water data from offshore Africa, we elaborate further with a sequence of first arrival modeling after tuned repositioning of sources and receivers at the sea floor.

## Introduction

Anisotropy is a key factor for the success of FWI when using long offset data from a surface seismic experiment. Prieux et al (2011) showed the importance of reconciling the kinematics of diving and reflected waves. Indeed, if not properly handled, the resulting FWI model may not optimally flatten CIGs even with an excellent fit between observed and computed diving waves (Mothi and Kumar, 2014). Anisotropy estimation through FWI has been studied and implemented for several years. The main difficulty appears to be the intrinsic coupling of velocity and anisotropic parameter spaces associated with their differences in spatial wavelength coverage (emphasized for example in Alkhalifah and Plessix (2014)). Several works discuss the right choice of parameters to use in order to improve the conditioning of the inverse problem, such as Plessix and Cao (2011), Gholami et al (2013) or da Silva et al (2014). From the results shown in these publications it appears that, while similar to amplitude versus offset or angle analysis (AVO, AVA) there is some hope to decouple two parameters for the short wavelengths, there is far less evidence to succeed for the longest wavelengths. Although there have been several attempts to perform anisotropic FWI, their success remains limited and conditioned to some prior information appearing in the initial model, model parameterization or constraints in the cost function (Stopin et al., 2014, Ramos-Martinez et al. 2017). As an example, Debens et al (2015) alternate a global optimization for anisotropy with a local optimization for the velocity. They succeed in retrieving both long wavelengths of velocity and anisotropy, but on an example where the starting model already contains all the long wavelength components of the velocity model.

The great difficulty of decoupling the long wavelength components of velocity and anisotropy (typically NMO velocity  $V_n$  and anellipticity  $\eta$  while fixing Thomsen's parameter  $\delta$ ) comes from the fact that conventional FWI is mainly driven by the kinematics of diving waves (Mothi and Kumar, 2014). In terms of information, it then mainly consists of one travel time by shot and receiver pair, which can be interpreted by a single parameter velocity model (Plessix and Cao, 2011). A solution could then invert the anisotropic velocity model from both reflection and transmission data jointly with a full wave approach driven both by the kinematic of diving and reflected waves (Zhou et al., 2015). With this aim, Djebbi et al (2017) analyzed the associated full wave traveltime sensitivity kernels. While such approaches could offer a practical solution in the future, they are still facing all the issues encountered with full wave tomography and multi-parameter full wave inversion.

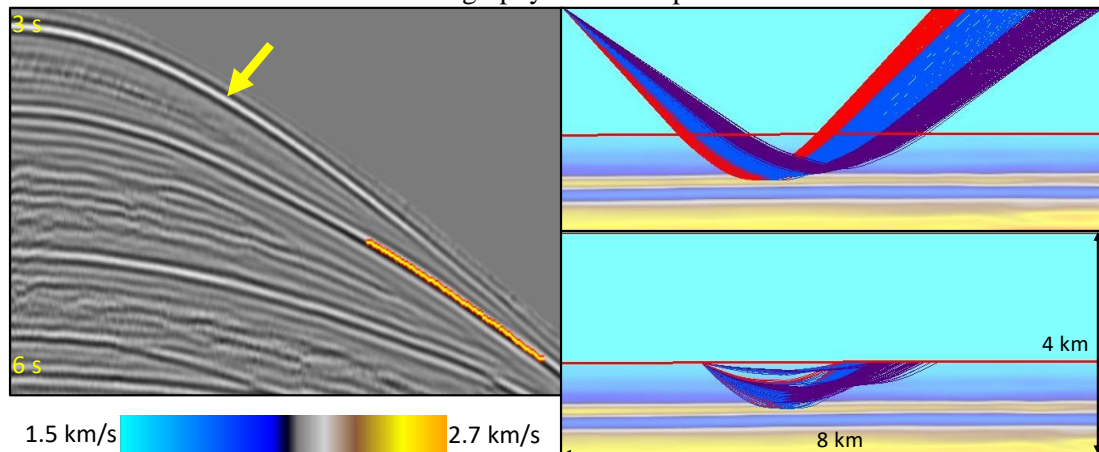


Figure 1: Computed first break traveltimes from an initial FWI velocity model explaining the kinematics of diving waves. Left: shot gather for observed data overlaid with computed diving wave traveltimes, the arrow points out the water bottom reflection. Top right: diving ray trajectories, Bottom right: diving ray trajectories for fictitious sources and receivers located on the seabed, spanning the same portion of the subsurface.

In this context, Allemand et al (2017) developed a ray-based version of this joint reflected and diving wave tomographic inversion. It consisted in using first arrival traveltimes and reflection curvatures in a nonlinear tomography to update  $V_n$  and  $\eta$  or similarly the vertical velocity  $V$  and Thomsen's parameter  $\epsilon$  and illustrated with a successful application on a 3D land dataset. But while reflection curvature picking is routinely performed in depth model building, first arrival traveltime picking is not

so common: it is usually done only for land data on short offsets to compute weathering zone statics. It can be a very tedious task and is clearly the bottleneck of the method. We propose in this study to accomplish this task with a modelling step that requires much less manual work. Indeed, before considering an anisotropy update, a first FWI update is often done and the resulting model correctly reproduces the kinematics of the observed diving waves. Consequently, it contains all requirements to generate the first arrival traveltimes; all we need to do is to extract them using for example an eikonal solver. We detail here this innovative workflow and show an application on a 3D real marine dataset.

### New workflow for anisotropy estimation

Based on the analysis above we propose the following workflow:

- 1) Run an initial FWI with diving waves, updating one parameter only, until the modelled data correctly matches the observed ones,
- 2) Use the output model to compute first arrival traveltimes between sources and receivers (Figure 1), using for example an eikonal solver,
- 3) Use these traveltimes together with RMO picks as an input to the joint reflection-diving wave tomography proposed by Allemand et al (2017), updating two parameters such as  $V$  and  $\varepsilon$  or  $V_n$  and  $\eta$ ,
- 4) Use the result (both velocity and anisotropy, or just the anisotropy) as an initial model for a final FWI, updating one or two parameters.

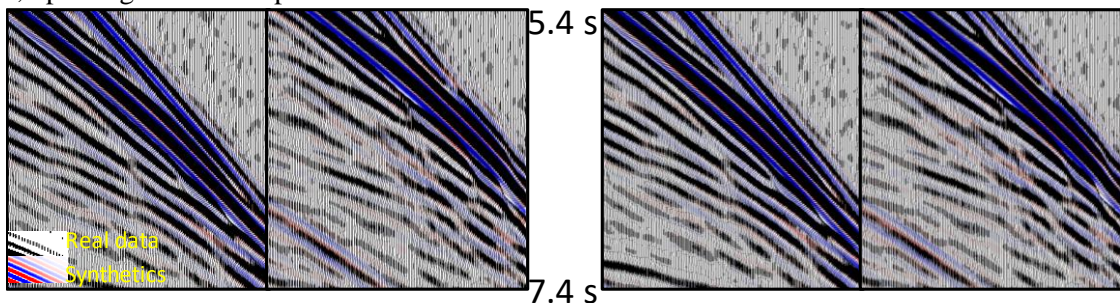


Figure 2: QC of initial (left) and final FWI (right) after 9 Hz FWI. Offsets vary from 4.2 km to 8.2 km.

Note that in the second step, one does not have to follow the real acquisition geometry. Indeed, it is possible to locate fictitious sources and receivers somewhere in the model as soon as the associated ray paths fit with the ones inverted by the initial FWI. In the case of an ocean bottom acquisition, for example, as the water velocity is known quite well, it is interesting to use fit for purpose source and receiver positions located at the seabed. Minimum and maximum offsets have to be selected to match the ray paths of surface data. The advantage of this repositioning is that we can use diving waves arriving later than the first arrival in the observed data (Figure 1 top). The maximum frequency inverted in the initial FWI is certainly another important parameter of our workflow. It impacts the accuracy of our first break estimation and will determine the level of homogenization of the heterogeneous velocity model by propagated waves. In practice, we usually run FWI with a maximum frequency of 8 to 10 Hz which insures some stability to the calculated traveltimes while capturing the kinematics of the main energetic arrivals (Figure 1).

### Real data example

The data we used comes from a 900 km<sup>2</sup> subset of a 3D marine dataset acquired offshore Africa with a spread of 10 streamers separated by 150 m. The hydrophones are distributed every 12.5 m along the 8 km cables and the dual-source separation is 18.75 m. In order to leverage the latest broadband technologies the streamers are deployed with a variable depth configuration. Starting from a smooth, almost 1D, velocity model derived from the PSTM velocities, we ran an initial FWI up to 9 Hz to update the velocity, using a constant anisotropy ( $\delta=3\%$  and  $\varepsilon=5\%$  below the water bottom). We can see on Figure 2 (left) that the match between synthetic and real data is good for the early arrivals, while the CIGs displayed in Figure 3 (left) are mostly curving down. This indicates that the velocity estimated by FWI is not properly scaled, and generally faster than the vertical velocity; hence, we should update the anisotropy.



We decided to update the anisotropy with the workflow presented in the previous section and in particular with the introduction of relocated source and receiver positions at the sea bottom (Figure 1). As mentioned earlier, it is interesting to note that the considered arrival is not the first break in the data: it comes after the direct arrival and the water bottom reflection. We then ran joint reflection-diving wave tomography using the computed first arrival times and picked RMOs on reflected events while jointly updating  $V$  and  $\epsilon$ . Initial  $\delta$  and  $\epsilon$  were 3% and 5% below the water bottom, respectively. We kept  $\delta$  unchanged during the whole process since it causes mostly a depth stretching effect, which requires well information to constrain it. The magnitude of  $\epsilon$  model obtained after joint tomography (Figure 4) has been increased with respect to its initial value, which is compatible with the fact that initial CIGs were mostly curving down.

Finally, using the updated  $\epsilon$  model by the joint tomography, we ran a velocity update with FWI up to 9 Hz. Figure 2 shows the match between synthetic and real data after initial FWI (using constant  $\epsilon$ ) and final FWI (using inverted  $\epsilon$ ). Both are similarly acceptable, because FWI performs well in both cases. Figure 3 compares the CIGs migrated with the constant  $\epsilon$  and inverted  $\epsilon$  FWI models. The process has significantly improved the flatness of the CIGs. We are therefore confident in the success of the decoupling between vertical and horizontal velocity by the proposed workflow, which is confirmed by comparing the  $\epsilon$  field (proxy for the horizontal velocity) and the velocity model after the final FWI (Figure 4, right): the high anisotropy values do not necessarily match the high velocity zones. A zoom on the migrated stack section is visible on Figure 5 for both the constant  $\epsilon$  and inverted  $\epsilon$  FWI. The new workflow has improved the focusing of the reflection events, especially in the faulted area, leading to a better image.

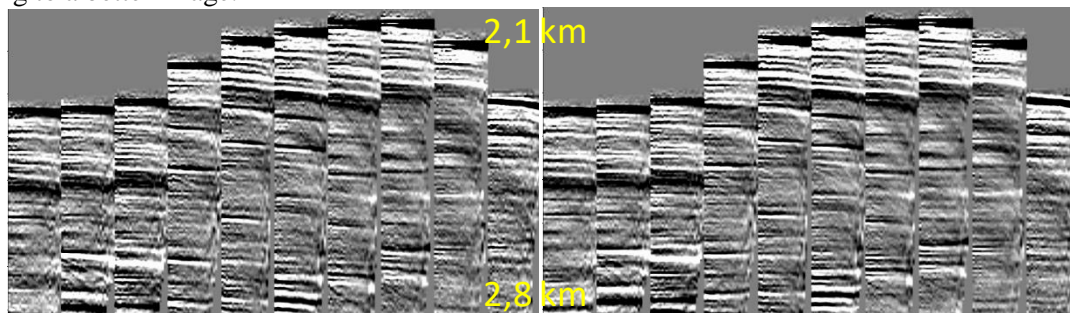


Figure 3: CIGs spaced evenly along an inline section, computed in the 9 Hz FWI model with constant  $\epsilon$  (left), and in the 9 Hz FWI model using inverted  $\epsilon$  (right).

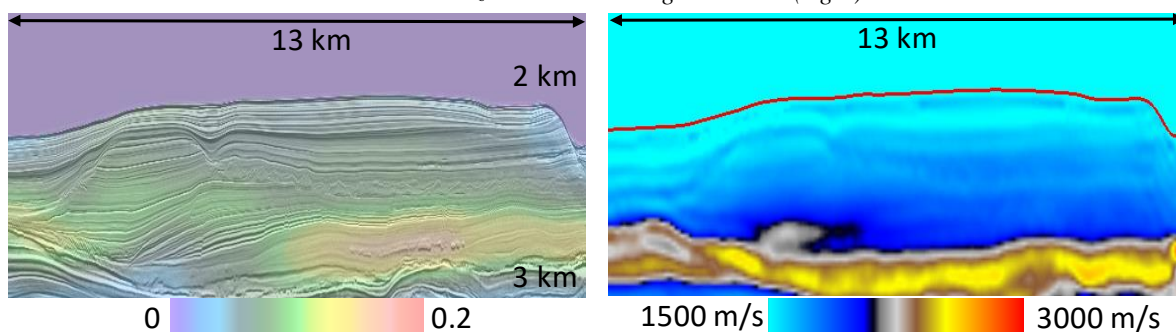


Figure 4: updated  $\epsilon$  model by joint reflection-diving waves tomography (left), 9 Hz FWI velocity model using inverted  $\epsilon$  from joint tomography (right)

## Conclusion

FWI is an excellent tool for velocity model building; however, when dealing with anisotropic media, it is not able to resolve for both velocity and anisotropy on its own. This is because it mainly relies on diving waves, which can be explained by only one parameter. We propose an innovative robust workflow solving this issue that includes a first pass of FWI to estimate velocity with constant anisotropy, traveltimes modelling to generate the first arrivals, joint reflection-refraction tomography to update anisotropy and then the final FWI. The effectiveness of this workflow is demonstrated on a real 3D dataset using deep water data, for which an additional step of source and receiver repositioning was used. In the future, the joint reflection-refraction tomography step could be replaced

by FWI jointly using the diving waves and the kinematics of the reflections, which would offer the possibility to use all of the diving waves instead of selecting only one arrival.

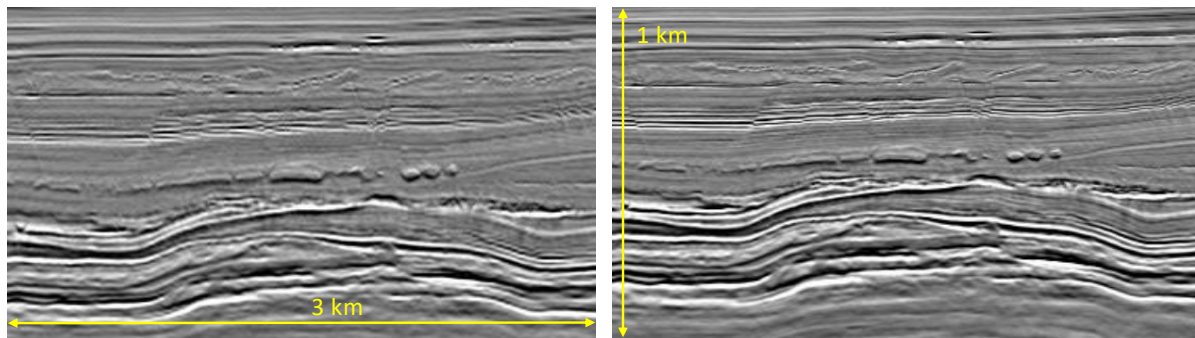


Figure 5: Migrated stack section after 9Hz FWI using constant  $\epsilon$  (left), using inverted  $\epsilon$  (right)

### Acknowledgement

We acknowledge CGG for permission to publish this work.

### References

- Alkhalifah, T., and Plessix, R. É. [2014] A recipe for practical full-waveform inversion in anisotropic media: An analytical parameter resolution study. *Geophysics*, **79**(3), R91-R101.
- Allemand, T., Sedova, A., and Hermant, O. [2017]. Flattening common image gathers after full-waveform inversion: The challenge of anisotropy estimation. *87<sup>th</sup> SEG Annual Meeting*, Expanded Abstracts, 1410-1415.
- da Silva, N. V., Ratcliffe, A., Conroy, G., Vinje, V., and Body, G. [2014]. A new parameterization for anisotropy update in full waveform inversion. *84<sup>th</sup> SEG Annual Meeting*, Expanded Abstracts, 1050-1055.
- Debens, H. A., Warner, M. R., and Umpleby, A. [2015]. Global anisotropic FWI. *77<sup>th</sup> EAGE Conference and Exhibition*, Extended Abstracts.
- Djebbi, R., Plessix, R. É., and Alkhalifah, T. [2017]. Analysis of the traveltimes sensitivity kernels for an acoustic transversely isotropic medium with a vertical axis of symmetry. *Geophysical prospecting*, **65**(1), 22-34.
- Gholami, Y., Brossier, R., Operto, S., Ribodetti, A., and Virieux, J. [2013]. Which parameterization is suitable for acoustic vertical transverse isotropic full waveform inversion? Part 1: Sensitivity and trade-off analysis. *Geophysics*, **78**(2), R81-R105.
- Mothi, S., and Kumar, R. [2014]. Detecting and estimating anisotropy errors using full waveform inversion and ray-based tomography: A case study using long-offset acquisition in the Gulf of Mexico. *84<sup>th</sup> SEG Annual Meeting*, Expanded Abstracts, 1066-1071.
- Plessix, R. E., and Cao, Q. [2011]. A parametrization study for surface seismic full waveform inversion in an acoustic vertical transversely isotropic medium. *Geophysical Journal International*, **185**(1), 539-556.
- Prieux, V., Brossier, R., Gholami, Y., Operto, S., Virieux, J., Barkved, O. I., and Kommedal, J. H. [2011]. On the footprint of anisotropy on isotropic full waveform inversion: the Valhall case study. *Geophysical Journal International*, **187**(3), 1495-1515.
- Ramos-Martinez, J., Qiu, L., Valenciano, A., and Shi, J. [2017]. An effective multiparameter full-waveform inversion in acoustic anisotropic media. *87<sup>th</sup> SEG Annual Meeting*, Expanded Abstracts, 1405-1409.
- Stopin, A., Plessix, R. É., and Al Abri, S. [2014]. Multiparameter waveform inversion of a large wide-azimuth low-frequency land data set in Oman. *Geophysics*, **79**(3), WA69-WA77.
- Zhou, W., Brossier, R., Operto, S., and Virieux, J. [2015]. Full waveform inversion of diving & reflected waves for velocity model building with impedance inversion based on scale separation. *Geophysical Journal International*, **202**(3), 1535-1554.